An Adaptive Front-end Readout System for Radiation Detection

Xiao Yun and Milutin Stanaćević
Department of Electrical and Computer Engineering
Stony Brook University, NY, USA
Email: xyun, milutin@ece.sunysb.edu

***Abstract*— A design of adaptive front-end preamplifier for measurement of optical response of epitaxial photodiode, registering light produced by semiconductor scintillator, is presented. A time constant of continuous-time based pulse shaping filter is adaptively determined to achieve optimal sensitivity for variable parameters of photodetector and readout electronics. Experimental prototype was designed in 0.5μm CMOS process.**

I. Introduction

Significant efforts have been made recently to enhance the effectiveness of nuclear and radiological detection capabilities, specifically in design of portable systems. A proposed three-dimensional (3D) integration of scintillation-type semiconductor detector pixels provides accurate spectroscopic resolution for isotope discrimination and an accurate determination of the direction to source at the same time [1]. In novel scintillation-type semiconductor detector high energy radiation produces electron-hole pairs in a direct-gap semiconductor material that subsequently undergo interband recombination, producing infrared light to be registered by a photo-detector. To measure the optical response of pixelized detector, an application specific integrated circuit has to be integrated with the array of detectors.

A significant design challenge for the ASIC is to minimize the equivalent input noise and achieve detection of small amount of input charge. However, the design parameters for minimum noise are greatly effected by the variability in the parameters of the detector, such as the parasitic capacitance and the leakage current. This paper proposes an adaptive solution that can be incorporated in the system to compensate for the variations of the detector and readout circuitry.

II. Readout System for Radiation Detection

Readout circuitry is directly interfaced to the photodiode and produces a voltage signal proportional to the total charge created by the scintillator in a single radiation event. The photodiode input can be modeled as a short charge pulse and associated parallel capacitance, proportional to the area of the photo-detector. Figure 1 shows a single channel block diagram of the proposed pixelated system. The system consists of charge sensitive amplifier(CSA), pulse shaper, peak detector, analog-to-digital converter(ADC) and adaptive control block. CSA provides low-impedance input node and integrates charge generated by photodiode on a small integrating capacitor in the feedback loop. Pulse shaper performs optimization of signal-to-noise ratio and in this implementation is realized as bandpass filter. Output signal of the shaper is a Gaussian shaped pulse, with peak proportional to the input charge and duration equal to the time constant of the shaper. Peak detector captures the amplitude of the pulse, that is converted to the digital value for detected radiation event. Adaptive control block produces threshold level for discrimination of radiation event. Adaptive control block also generates the time constant for the shaper, optimized for minimum output noise and increased sensitivity of the system.

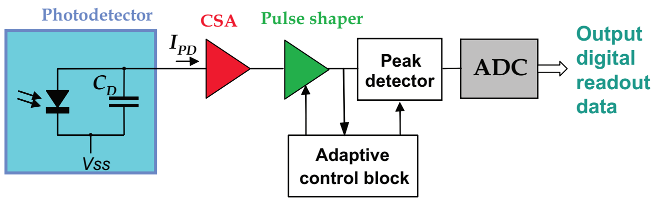

Fig. 1. Block diagram of proposed system

A. System design

The charge pulse of the photodiode has to be pre-amplified before any processing that is necessary for increased sensitivity and signal-to-noise ratio could take place. The input pre-amplification can be performed in two ways. The charge can be directly integrated on the detector capacitance and capacitor voltage can be recorded with high-input impedance voltage amplifier. In case of large detector capacitance, the direct integration of the charge on the detector capacitance would lead to undetectable voltage signal. Second option is to use a low input impedance amplifier, implemented through either charge or current amplifier. The charge amplifier leads to lower achievable sensitivity [2].

With charge sensitive amplifier, shown in Figure 2, charge is integrated on a small feedback capacitance C_f. In case of radiation event, created charge produces a voltage step signal at the output with an amplitude equal to approximately Q/C_f. Output signal of CSA would ideally be a step function due to short duration (10-100 ns) of input charge pulse. However, since a DC feedback is necessary for proper operation of amplifier, a resistance has to be added in the feedback loop. The resistance provides an exponential decay of the output signal. For the minimum input noise, the feedback resistance has to be as high as possible. The high resistance is realized using MOS

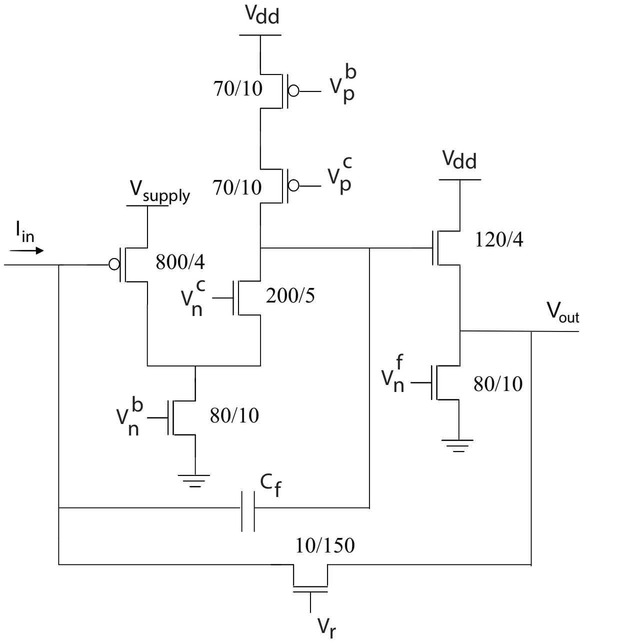

Fig. 2. Circuit implementation of CSA

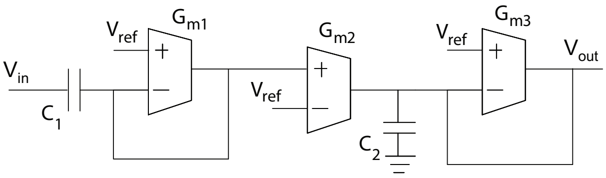

Fig. 3. Continusous-time bandpass filter implementation of shaper.

transistor biased in subthreshold region of operation. The high-gain amplifier is implemented as folded-cascode amplifier.

A continuous time Gm-C filter implements the pulse shaper, as shown in Figure 3. It is a first order differentiator cascaded with a first order integrator. The transfer function of the filter is

$$H(s) = \frac{G_{m2}}{G_{m3}}[\frac{sC_1/G_{m1}}{1+sC_1/G_{m1}}][\frac{1}{1+sC_2/G_{m3}}] \qquad (1)$$

G_{m1} and G_{m3} are nominally set to equal values. G_{m1}/C sets the time constant. The ratio of G_{m2} and G_{m3} sets the gain of the filter. Through change of biasing current, and subsequent change of transconductance g_m, the time constant of pulse shaper is adjusted.

B. Noise performance

Noise analysis of readout system is based on the assumption that the dominant noise sources are the shot noise of photodiode and noise (thermal and flicker noise) of the input MOS transistor. The input MOS transistor dominates the noise introduced by the readout electronics due to subsequent signal amplification and its optimization leads to optimal sensitivity. Equivalent noise charge (ENC) quantifies sensitivity of the system. ENC is defined as the ratio of the total integrated rms noise at the output of the pulse shaper to the signal amplitude due to one electron charge q [3].

The input equivalent voltage noise source of folded-cascode amplifier, V_n^2, and the shot noise from detector leakage current I_n^2 can be expressed as:

$$V_n^2 = \frac{8}{3}kT\frac{1}{g_m} + \frac{K_f}{C_{ox}WLf} \qquad (2)$$

$$I_n^2 = 2qI_o \qquad (3)$$

where g_m is the transconductance of input transistor, K_f is the 1/f noise coefficient of the CMOS process, and I_o is the leakage current of detector. The total noise power at the output of CSA is

$$V_{nCSA}^2(s) = (\frac{C_{in}+C_f}{C_f})^2 V_n^2 + (\frac{1}{sC_f})^2 I_n^2 \qquad (4)$$

where C_{in} is the capacitance seen at the input of CSA and is composed of the parasitic capacitance of detector and the parasitic input capacitance of CSA.

The transfer function of semi-Gaussian pulse shaper, consisting of one differentiator and n integrators, with the same time constant τ, is

$$H(s) = [\frac{s\tau}{1+s\tau}][\frac{1}{1+s\tau}]^n. \qquad (5)$$

The total noise power spectrum at the output of pulse shaper is:

$$V_{n,tot}^2 = \int_0^\infty |V_{nCSA}(j2\pi f)|^2 |H(j2\pi f)|^2 df \qquad (6)$$

The input signal due to one electron charge, q, generated from the detector can be modeled as a Dirac current pulse. The response to one electron is calculated as:

$$V_{out}(t) = \frac{qn^n}{C_f n!}(\frac{t}{n\tau})^n e^{-t/\tau} \qquad (7)$$

The above equation describes a semi-Gaussian alike pulse and has a peak at time $n\tau$. The peak amplitude is derived as:

$$V_{outmax} = \frac{qn^n}{C_f n! e^n} \qquad (8)$$

Thus, the peak amplitude of the output signal is linear with the generated charge and does not depend on the time constant of the shaper. By measuring the peak value of output signal, the amount of electrons that are generated from detector can be determined.

The ENC is then calculated as the signal divided by total noise at the output of shaper

$$ENC_{th}^2 = \frac{8}{3}kT\frac{1}{gm_1}\frac{C_{in}^2 B(\frac{3}{2}, n-\frac{1}{2})}{q^2 4\pi\tau}(\frac{n!^2 e^{2n}}{n^{2n}}) \qquad (9)$$

$$ENC_f^2 = \frac{K_f}{C_{ox}W_1L_1 f}\frac{C_{in}^2}{q^2 2n}(\frac{n!^2 e^{2n}}{n^{2n}}) \qquad (10)$$

$$ENC_o^2 = 2qI_o\frac{\tau B(\frac{3}{2}, n-\frac{1}{2})}{q^2 4\pi}(\frac{n!^2 e^{2n}}{n^{2n}}) \qquad (11)$$

where ENC_{th}, ENC_f, ENC_o represent contribution to ENC by thermal noise, 1/f noise and shot noise, respectively. $B()$ is

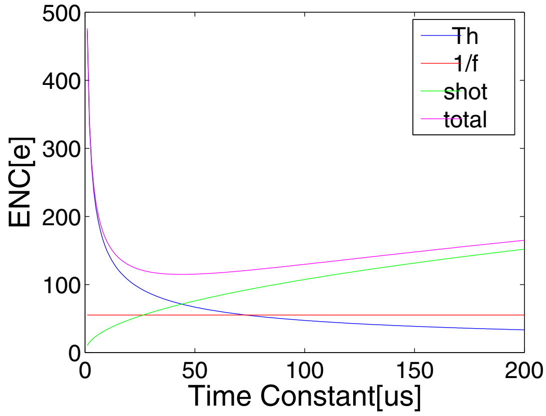

Fig. 4. ENC versus time constant

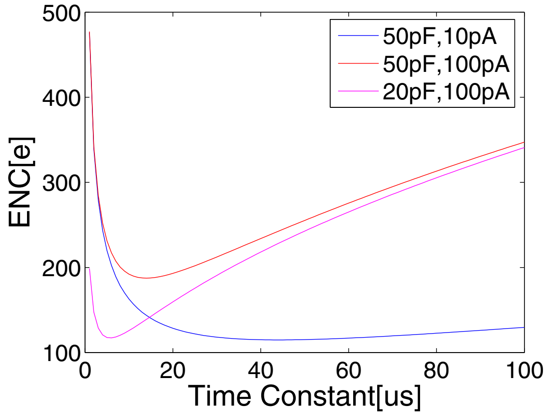

Fig. 5. ENC versus different specs

beta-function. The thermal noise component is proportional to input parasitic capacitance and inversely proportional to the peaking time of pulse shaper; the shot noise component is proportional to the peaking time; the 1/f noise component is proportional to input parasitic capacitance.

From above analysis, there exists an optimal time constant for any set of detector parasitic capacitance and leakage current. Figure 4 shows the calculated total ENC as well as three different components based on $50pF$ input capacitance and $10pA$ leakage current. Figure 5 shows the total ENC under different detector specifications.

III. Adaptive Control of Noise and Detection Level

The adaptive control block is used for optimization of noise performance of system through control of biasing current of OTA in shaper. This block, whose diagram is shown in Figure 6, also includes circuitry for optimal setting of the threshold value for comparison with peak detector signal in process of detection of radiation event and subsequent triggering of analog-to-digital conversion.

The variations in the leakage current of the photodiode can be significant, as well as the parameters of the input transistor.

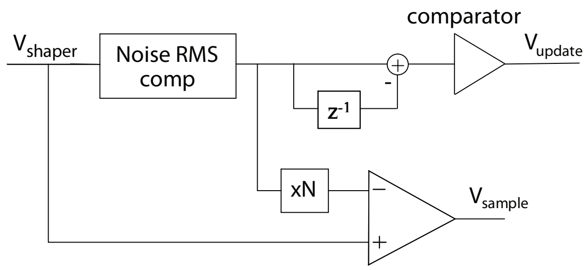

Fig. 6. Block diagram of adaptive noise processing

These variations affect the optimal performance of the pulse shaper, as shown in figure 5. As shown in equation (8), the amplitude of pulse shaper signal does not depend on time constant of shaper. The minimization of ENC with respect to time constant can then be achieved by minimization of the standard deviation of the output noise signal of the shaper. The output noise signal dependance on time constant of shaper can be written as

$$V_{n,tot}^2 = A/\tau + B\tau + C \quad (12)$$

where A, B and C are constants that depend on the parameters of the diode and readout circuitry.

To optimize the time constant of shaper, we propose adaptation based on stochastic perturbation technique [4]. A noise RMS computation block senses the RMS level of output signal from pulse shaper, $V_n(t)$. Based on the sign of the gradient of $V_n(t)$, obtained as difference between $V_n(t+T)$ and $V_n(t)$, a small increment of biasing current is performed, where the sign of constant increment depends on the sign of gradient. To demonstrate the algorithm, we have constructed an artificial output noise signal, which includes 1/f noise, thermal noise and shot noise components, in time domain. The thermal and shot noise are white and follow a Gaussian distribution in the time-domain. The time-domain 1/f noise is generated as described in [5]. Figure 7 shows a simulation of the proposed system. The red curve is the calculated ENC versus time constant, and the blue curve shows how the algorithm converges in an effort to optimize the value of time constant and minimize noise.

To generate the optimal detection level, an adaptive real-time threshold computation is used, with the threshold value equal to the multiple (N in Figure 6, usually 3 to 7) of the output noise standard deviation value. For computation of standard deviation of noise signal, a circuit proposed in biomedical applications for spike detection [6] was used.

IV. Results

The system was simulated using Cadence SpectreS simulator and BSIM3 version 3.1 transistor models. To demonstrate the performance of system, the input pulse is swept from equivalent input charge of 1,000 electrons to 100,000 electrons and output voltage is shown in figure 8. The simulated frequency response of the designed filter for pulse shaping is shown in Figure 9. It demonstrates how time constant of the shaper can be changed by change in the biasing voltage.

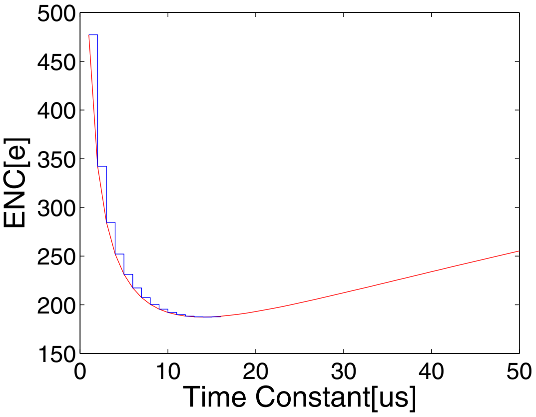

Fig. 7. Simulation of adaptive noise processing

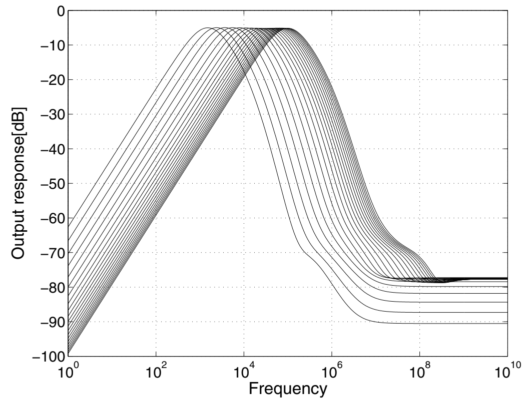

Fig. 9. Frequency response of the designed pulse shaper for variation of biasing voltage of OTA from 3.8 V to 4.2 V in steps of 200 mV

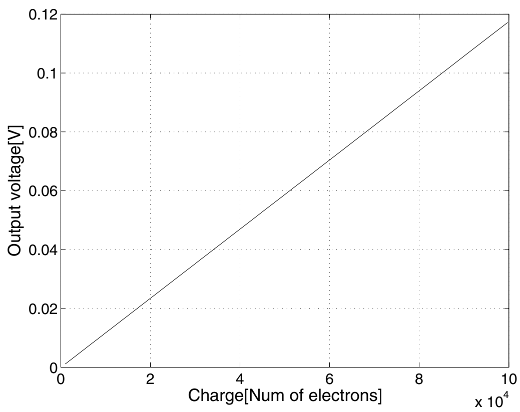

Fig. 8. Output voltage of the system as function of input charge

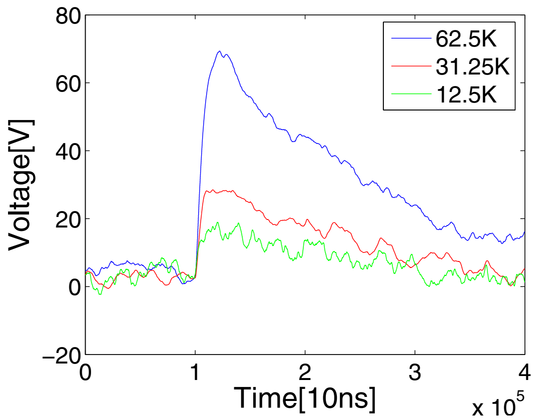

Fig. 10. Output of CSA for different input signals.

The biasing voltage of OTA is varied from 3.8 V to 4.2 V in steps of 200 mV. The time constant of the filter is changed from 1 us to 50 us.

The proposed system was implemented in 0.5 um CMOS technology. For characterization of the circuit without a sensor, a 1 pF capacitor is connected serially to the input of the CSA. Capacitor enables controlled charge injection into the readout circuitry, as the current pulse at the input is generated by applying a known voltage step signal to capacitor. The voltage step is applied using function generator. Figure 10 shows a response of CSA for different voltage steps: 2 mV, 5 mV and 10 mV. These voltage steps correspond to the total injected charge of 12.5 k, 31.25 k, and 62.5 k electrons, respectively.

V. Conclusion

This work presents a design of an adaptive recording system for radiation detection using semiconductor scintillator. The proposed system provides ability to minimize noise with variability in the photodiode and readout electronics. The adaptive control block automatically adjusts read out threshold based on the output noise level, thus giving the system potential for further programmability.

VI. Acknowledgments

This work is supported by the Domestic Nuclear Detection Office (DNDO), Department of Homeland Security.

References

[1] A. Kastalsky, S. Luryi and B. Spivak, “Semiconductor high-energy radiation scintillation detector,” Nucl. Instr. Meth. Phys. Res. A 565, pp. 650-656 (2006).

[2] S. Tedja, J. Van der Spiegel, H. H. Williams, “A CMOS Low-Noise and Low-Power Charge Smapling Integrated Circuit for Capacitive Detector/Sensor Interfaces”, IEEE J. of Solid-State Circuits, vol. 30,No. 2, November 1995.

[3] W.M.C. Sansen, Z.Y. Chang, “Limits of Low Noise Performance of Detector Readout Front Ends in CMOS Technology”, IEEE Transactions on Circuits and Systems, vol. 37, No. 11, November 1990.

[4] G. Cauwenberghs, “A Fast Stochastic Error-Descent Algorithm for Supervised Learning and Optimization”, Adv. Neural Information Processing Systems (NIPS*92), San Mateo, CA: Morgan Kaufman, vol. 5, pp. 244-251, 1993.

[5] T.-H. Lee and G. Cho, “A Monte Carlo based time-domain Hspice noise simulation for CSA-CR RC circuit”, Nuclear Instruments and Methods in Physics Research A(505), pp. 328-333, 2003.

[6] R. R. Harrison, “A Low-Power Integrated Circuit for Adaptive Detection of Action Potentials in Noise Signals”, Proceedings of the 25th Annual International Conference of the IEEE EMBS, Cancun, Mexico, September 17-21, 2003.